Journal of Critical Reviews

ISSN- 2394-5125 Vol 7, Issue 4, 2020

Review Article

# APPLICATION OF BIO-WASTE MATERIALS IN THE GREEN SYNTHESIS OF COMPOSITES FOR WATER PURIFICATION

**K. Jayaraj[1], M. Suriya[2], Anitha Pius[3]**

[1]Department of Chemistry, The Gandhigram Rural Institute- Deemed to be University, Gandhigram, Dindigul, Tamil Nadu, India.
[2]Department of Chemistry, The Gandhigram Rural Institute- Deemed to be University, Gandhigram, Dindigul, Tamil Nadu, India.
[3]Department of Chemistry, The Gandhigram Rural Institute- Deemed to be University, Gandhigram, Dindigul, Tamil Nadu, India.

*Received: 19.12.2019* *Revised: 07.01.2020* *Accepted: 05.02.2020*

**Abstract**

Treatment of the polluted water has become an issue of cardinal importance in the framing of the most recent strategies that define the way the environmental engineering and conservation are being looked upon. Adsorption techniques that involve solid adsorbents have been widely practiced to filter out the contaminants from the aqueous contents, and composites of biopolymer have attracted greater attention because they are inherently innocuous to the environment and can be classified as bio-degradable. Biopolymer-based nano-composites in particular have often been proved to be possessing better physical, chemical, and mechanical properties than those of the corresponding biopolymers as such, and also provide the advantages of both counterparts in the composites. This paper details versatile biopolymer-based composites of cellulose extracted from banana peel impregnated with zero-valent iron nanoparticles aimed at the discharge of an organ othiophosphate pesticide from aqueous contents. The prepared composites were characterised by scanning electron microscopy, Fourier-transform infrared spectroscopy, X-ray diffraction, and Brunauer–Emmett–Teller analysis. The synthesis of the adsorbents, their intrinsic adsorption characteristics, and effective applications are the focal point of this paper and are subjected to detailed analysis.

***Keywords:*** Adsorption, Phosphate, nanoscale Fe(0), cellulose

***Highlights***

- Broad Applicability: Useful for removing various micropollutants
- Low-cost: The cellulose is obtained from a waste material that is widely available.
- Eco-friendly: Does not harm the environment since the matrix is biodegradable cellulose

 DOI: http://dx.doi.org/10.31838/jcr.07.04.52

## INTRODUCTION

Water is a fundamental resource that sustains life. The main accessible drinkable fresh water is the ground water. Water quality is a significant factor that affects human life and contamination of water is a noteworthy worldwide issue that requires continuous assessment.

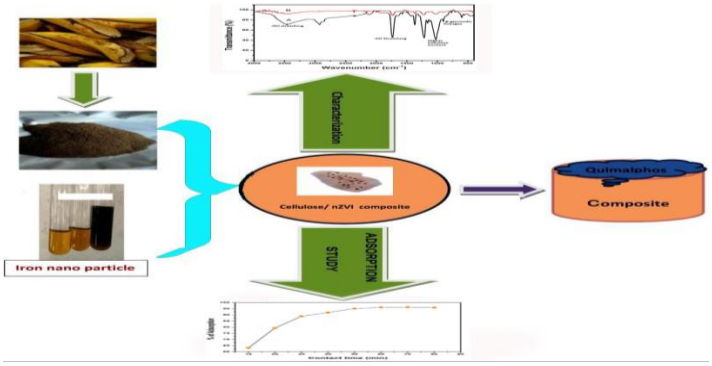


On account of the unbridled utilisation of toxins and their passage into water bodies, it is important to develop the most efficient methods that will help to eliminate them from water and thereby distil it [1]. Various strategies have been examined to eliminate poisonous materials from water, among which the most common methods are oxidation [2,3], ozonation [4-6], adsorption with activated carbon [7–10], nanofiltration [11–13], irradiation techniques [14], biological techniques [15,16], photocatalysis [17], Fenton treatment [18], ultrasonic treatment [19-21], and film-based adsorption [22-24]. Among these, adsorption is an outstanding and effective strategy for disinfecting water. Adsorption has been noted to be a better strategy than other strategies for water reutilisation in terms of the initial cost, flexibility, and ease of operation. Moreover, adsorption does not result in the production of harmful substances. Therefore, developing an effective sorbent and a simpler separation procedure would be advantageous for water remediation.

Cellulose is the amplest natural polymer that can be found in nature; it is sustainable, biodegradable, and biocompatible. Utilising cellulose is beneficial for manageable and long-term monetary interests [25]. Cellulose-based bionanocomposite is a typical term used to refer to the mixtures of nanomaterials of characteristic polymers doped with foreign species or without

doped with them, for example, organic or inorganic nanoparticles [26,27]. Apart from cellulose, other biopolymers such as proteins, polysaccharides, DNA, polyhydroxy alkanoates, and chitin/chitosan [28–34] are the major species included in biopolymer-based nanocomposites.

Recently, cellulose-based nanocomposites that have potential utility in differed fields including water purification have been attracting interest. The nanocomposites are generally composed of ferromagnetic particles discharged either in ferrous or non-ferrous framework [35]. Kadam et al. [36] applied chitosan-based nanocomposites for the adsorption of hazardous pollutants. Li et al.[37] created fungus-$Fe_3O_4$ bionanocomposites to dispense radioactive $UO_2^{2+}$ particles from atomic waste water.

In this study, we analyze the possibility of making use of a specialized adsorbent for the elimination of pesticides from aqueous solutions. Considering the severity of water contamination with pesticides and its effect on human beings, we utilised composites of cellulose derived from banana peel impregnated with iron nanoparticles as adsorbents for their removal. The results of analysis conducted on adsorption indicated that the nanocomposite of $Fe_2O_3$ and cellulose from banana peel has a higher adsorption limit of 96 $mg \cdot g^{-1}$. The adsorption was found to be happening at almost blistering pace, and the adsorption equilibrium was accomplished in under 5 min. Moreover, good phosphate-adsorption characteristics were observed at pH 7. Thus, the nanocomposite of cellulose separated from banana peel and $Fe_2O_3$ could serve as a suitable adsorbent for the riddance of phosphate from aqueous solutions.

## MATERIALS AND METHODS

### Chemicals and Materials

Every single chemical used here were of analytical grade and were obtained from SRL - Sisco Research Laboratories Pvt. Ltd., Mumbai, India. Phosphate stock solution was made from anhydrous potassium di hydrogen orthophosphate. All solutions were obtained using deionised water. The banana samples were obtained from the local market in Kerala, India.

### Methods

#### 1. Preparation of banana peel flour

The bananas were cleansed thoroughly by washing under the tap water, which was then followed by a detailed soaking in double distilled water for 1 hour to get rid of any dust or dirt sticking to the peel and then they were wiped dry using a tissue-paper. Subsequently, the cleaned bananas were subjected to manual peeling and the pulp was extracted from those peels. The peels were then immersed in a 1% potassium metabisulfate solution for 12 h to hinder oxidation and enzymatic browning. After that, the peels were subjected to desiccation at 50 °C for 24 h, ground, and passed through a 0.25 mm mesh. Finally, the ground powder was packed in polyethylene bags and stored at 4 °C until use (Fig. 1).

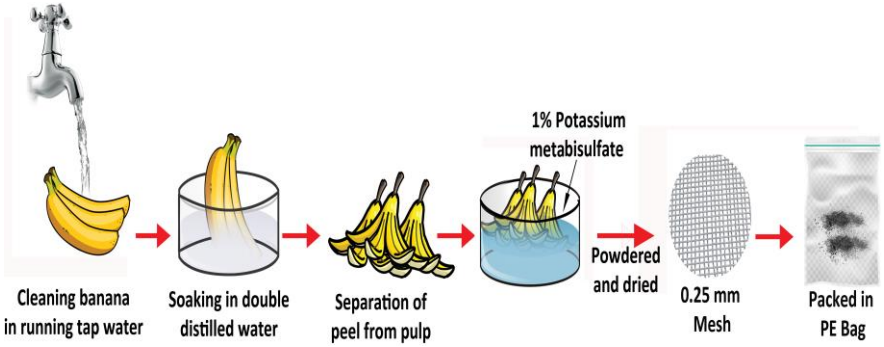


**Fig. 1: Schematic of the preparation of banana peel powder**

#### Isolation of cellulose fibres (CFs) as cellulose nanofibres

The banana fibre was subjected to alkali treatment using a solution comprised of 20% (w/v) sodium hydroxide and 0.1% anthraquinone at 170 °C for 1.5 h. Then, it was cleansed using distilled water to wash off pectin, lignin, and hemicelluloses. The insolvable pellet was further de-lignified with 15% (w/v) $NaClO_2$ [pH 5 balanced with acetic acid (10% (v/v))] at a temperature of 70 °C for 1 hour, and then it was washed. The bleaching was performed again by maintaining the same conditions to induce further effective decolourisation and lixiviating of phenolic compounds and lignins. Then, a second alkali treatment was carried out with 5% (v/v) potassium hydroxide at 25 °C for 1.5 h followed by washing to eliminate hemi cellulose. Finally, the insoluble pellet was hydrolysed using 15% (v/v) sulfuric acid at a temperature of 80 °C for 1 hour to leach out trace residual starch, minerals and hydrolysed amorphous-cellulose so as to obtain the cellulose in the nanofibre form. After each phase of the chemical treatment, the insolvable pellet obtained was washed using distilled water and then subjected to centrifuge at 10000 rpm at a temperature of 4 °C for 20 minutes until the pH of the pellet was neutralised (15).

#### Preparation of nanoscale zero-valent iron (nZVI)

One gram of ferric (II) chloride hexahydrate ($FeCl_3.6H_2O$) was dissolved in 50 mL of ethanol. The reducing agent, 1 g of sodium metaborohydride dissolved in 50 mL of deionised water, was dripped into the ferric chloride solution under manual swirling of the beaker. Blocks of agglomerated particles formed, indicating the formation of nZVI. After the complete addition of the borohydride solution, the mixture was allowed to settle for 15 min. It was then centrifuged and the separated particles were washed using ethanol and then subjected to vacuum-drying (16) (Fig. 2).

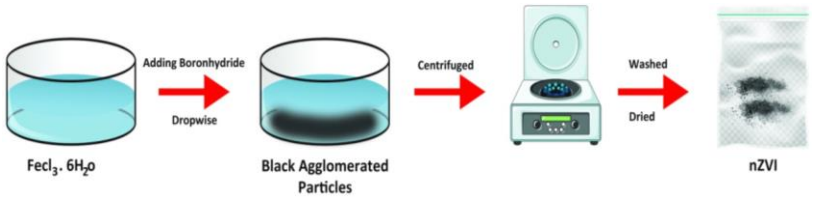


**Fig. 2 Preparation of nZVI – Processing Routes Overview**

**WATER-TREATMENT PARAMETERS**

The effect of contact time, pH value of the solution, contaminant-concentration, and adsorbent-dosage on the adsorption characteristics of the prepared ZVI/cellulose fibre (CF) composite were studied as follows:

**Effect of contact time**

Prepared adsorbent's adsorption efficiency (nZVI supported on cellulose from banana peel) during different contact times of 10 to 60 min. was analyzed. The leadoff concentration value of the stock solution, pH, and the adsorbent-dosage were ensured to stay constant.

**Effect of pH**

The adsorption-efficiency of ZVI/CF composite was analyzed for pH ranging from 3 to 11 by maintaining the leadoff concentration, contact-time, and the dose of the composite unchanged.

**Effect of the concentration**

The adsorption capacity of the composite was examined using quinalphos solutions of different concentrations ranging from 10–50 ppm. Here, pH, contact time, and dosage of the composite were made sure to stay unchanged.

**Dosage of adsorbent**

The percentage-removal of the contaminant for different dosages of the adsorbent viz., 0.1, 0.2, 0.3, 0.4, and 0.5g was analyzed to evaluate the impact of dosage and also to optimise the minimum dosage required for the elimination of quinalphos.

**Experimental set-up**

Studies on the removal of pesticide were conducted by shaking the ZVI/CFs composite prepared in 30 mL of the quinalphos solution at steady rate. The task was carried out at room temperature by employing a mechanical shaker. The samples were then retrieved at predetermined fixed time-intervals for the analysis of the quinalphos concentration. UV-visible spectrometer (Ultraviolet/visible Spectrometer Perkin Elmer Lambda USA) is the devise that was used to guage the concentration of the quinalphos solutions; the absorbance values of the solutions got gauged at 624, 554, and 663 nm sequentially. The concentration level of quinalphos solutions both prior to and post the adsorption process got quantified by making use of an Atomic-adsorption spectrometer (AAS; Perkin Elmer A Analyst 100).

The Removal-efficiency (%) of the quinalphos was determined using Eq. 3.

$$Removal\ \% = \frac{C_i - C_f}{C_i} \times 100 \quad (1)$$

where $C_i$ is the initial value of concentration and $C_f$ is the final value of concentration of the pollutant solution after being treated with the composite.

The Adsorption Capacity ($Q$) of the composite was calculated using Eq. 4

$$Q(mg\ g^{-1}) = \frac{(C_0 - C_t)V}{m} \quad (2)$$

where $C_o$ and $C_t$ are the initial and final value of the pollutant solution concentration, $m$ - the mass of the adsorbent, and $V$ - the volume of the content.

Adsorption experiments were conducted by introducing varying amounts of adsorbent, that is, nanoscale zero-valent iron (nZVI) supported on cellulose derived from banana peel was added to 50 mL volumes of quinalphos solutions of different concentrations. The mixtures were subjected to intense shaking at constant rate using a mechanical shaker at room temperature.

**CHARACTERISATION**

**Scanning Electron Microscopy (SEM)**

The morphology of the prepared composite before and after treatment was analyzed by SEM (*TESCAN vega*).

**Fourier Transform Infrared Spectrometer (FTIR)**

The structure of the nZVI/CF composite before and after the adsorption of quinalphos was studied by Fourier Transform-Infra Red (FT-IR) spectrometry (Jasco 460 plus model). The FT-IR spectrum of the composite was recorded over a wavelength of 500 to 4000 $cm^{-1}$ range by the KBr disk (thin pellets) method.

**X-ray diffraction (XRD) analysis**

The structure and phase of the synthesised composite were characterised by XRD (Bruker binary v3 X-rayDdiffractometer) with Cu Kα radiation (λ = 1.5406 Å) as the X-ray source, operated at a tube voltage of 40 kV and current of 30 mA. The patterns were collected in the range of 2θ = 10–80°.

The average crystallite size (D) of the composite was determined from the full-width-at-half-maximum (FWHM) of the main peak, using the Debye-Scherer formula,

$$D = \frac{0.9\lambda}{\beta cos\theta} \quad (3)$$

where D is the crystallite size, λ is the wavelength of the Cu Kα radiation, β is the FWHM in radians, and θ is the Bragg's angle.

**RESULTS AND DISCUSSION**

**Visual examination of the emergence of the CNF suspension**

The effects of each chemical treatment on the banana-peel flour during the segregation of CNFs could be easily visualized. The different stages of the process and the changes incurred in the colour of the peel flour after each treatment step owing to the leaching out of elements like lignin, pectin, tannin, proteins, starch, hemicelluloses, minerals etc., are illustrated in detail in Fig. 3. Initially the peel-flour colour was found to be darkish brown (post the first alkali treatment) which then switched to lighter brown (post the initial bleach treatment) and the gradual discoloration from brown to pure white was well underway all along the second bleaching, second alkali treatment, and acid hydrolysis steps. The alkali treatment process was conducted to hydrolyse and solubilise pectins, starch, hemicelluloses, and proteins (17), while the bleaching process was employed to expel lignins and tannins, which turned out to be the responsible factor for the appearance of the peel flour in brown colour (18). Bleaching process that was carried out with 1 percent $NaClO_2$ solution (pH 5) at the temperature of 70 °C for 1 hour facilitated the bleach of most of the lignins. Since chlorine and chlorites tend to oxidise lignin rapidly causing the generation of hydroxyl, carboxyl, and carbonyl groups that lead to the effective solubilisation of lignin in the alkaline medium, the cellulose was purified (17). Expulsion of lignin from plant sources using $NaClO_2$ is possibly the most familiar technique used in the laboratories (18). The photographs in Fig. 3 show the changes seen in the banana-peel flour-colour following various chemical treatments.

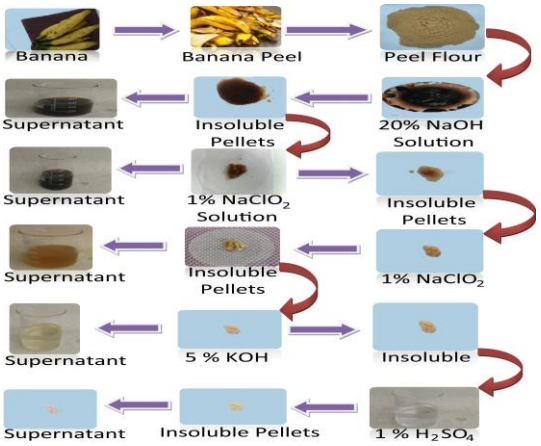


**Fig. 3: Photographs showing the phase-by-phase tarnishing or discoloration of peel flour during the segregation of cellulose fibres**

**Visualization of the microstructure by SEM**

The modifications in the structure of cellulose nanofibres after the chemical treatment processes were examined by SEM. The SEM images of the nanofibres were analogized with the SEM images of the banana peel (Fig. 4a-d), which aided us to decipher the structure of these fibres. The banana peel (Fig. 4a) exhibited an irregular structure and was found to be consisting of some starch granules. The process of chemical treatment culminated in elimination of amorphous-components such a lignin, hemi-cellulose and pectin (18). It's apparent that the chemical treatment, bleaching and the ultrasonic treatment implemented for the fragmentation of the obtained nanofibres (Fig. 4b–d) induced certain chemical and structural alterations in them.

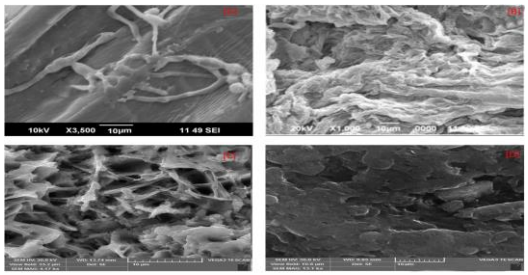

**Fig. 4 SEM images of a) banana peel and b) cellulose nanofibres obtained by various chemical treatments. c) nZVI/CFs from banana peel before the adsorption of quinalphos. d) nZVI/CFs from banana peel after the adsorption of quinalphos**

**FT-IR studies**

FTIR spectroscopy is a relevant technique to discover the changes in the chemical composition of the segregated samples after different treatments. The FT-IR spectrum of banana-peel cellulose nanofibres is exhibited in Fig. 5, where almost identical spectral characteristics are observed across the samples. Broadened absorption band characteristic of the –OH stretching was observed in the spectra in the region of range 3000-3650 $cm^{-1}$. The band observed at 3442 $cm^{-1}$ corresponds to intramolecularly hydrogen-bonded –OH groups in cellulose (19). The small peak observed at 2914 $cm^{-1}$, can be ascribed to the aliphatic saturated C–H stretching-vibration of the cellulose and the hemi celluloses (18); further, the waxes were deemed eliminated after the subsequent chemical treatments (20). The shoulder at 1732 $cm^{-1}$, which is barely present in all the spectra is ascribed to the vibrations of the acetyl and the uronic ester groups of the hemicelluloses or the ester linkages of the carboxylic group of the ferulic and p-coumaric acids of lignin and/or hemicelluloses (21). Its absence can be ascribed to the chemical treatment, by which the hemi celluloses and the lignin components contained in the sample were dissolved. The prominent band observed at 1635 $cm^{-1}$ represents the bending-mode of adsorbed water (22).

FT-IR studies of the banana peel reveal that in the 1608–1640 $cm^{-1}$ range, bands which quite often are observed were undetected in this study, which might be owing to the partial or the incomplete reaction process of the C–O bonds of hemicelluloses, which were bleached when the chemical treatment of the cellulose nanofibres was underway (18). The vibration at 1233 $cm^{-1}$ can be attributed to the C–O stretching of the guaiacyl ring. The two peaks observed at 1554 and 1375 $cm^{-1}$ indicate aromatic C–C stretching vibrations of the aromatic ring of lignin. The prominent band of the skeletal stretching vibration of the C –O-C pyranose-ring at 1030 $cm^{-1}$ was noticeable in all the 4 spectrums, indicating the presence of xylans associated with hemi-celluloses, confirming that xyloglucans were strongly binding to the cellulose nanofibres. Furthermore, the intensity of this band demonstrates the presence of higher content of cellulose in chemically treated cellulose nanofibres (20,21). A less intense band at 920 $cm^{-1}$ can be ascribed to the C–O stretching, which has apparently dissolved along with the chemical treatment process (23). A sharp band was observed at 850 $cm^{-1}$ across the spectra of cellulose nanofibre samples, which represents the classic cellulose structure. This band is ascribed to glycosidic hydrocarbon deformation with the ring vibration of –OH bending and it testifies to the obvious presence of β-glycosidic linkages between the anhydrous glucose units of cellulose (24).

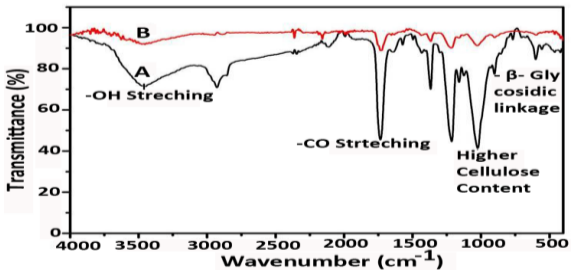


**Fig. 5: FT-IR spectra of A) nZVI/cellulose acetate/CF composite before the adsorption of quinalphos and B) after the adsorption of quinalphos**

**X-ray diffraction (XRD)**

The crystallinity factor of cellulose is highly significant since it determines its tendencies. The XRD pattern of the cellulose nanofibres extracted from banana peel was recorded to investigate its crystallinity. The XRD pattern clearly shows acute peaks at $2\theta$ = 16° and 22°, which represent the idiosyncratic diffraction peaks of cellulose, suggesting the good crystallinity of nanofibres (25). The results indicate that during the chemical treatment, the structure of cellulose which is crystalline in nature seldom changed. The Crystallinity-index ($I_c$) got estimated using Eq. (1) is 30.50, 44.14, 50.74, and 63.64% for 0, 400, 800, and 1000 W, respectively (Fig. 6).

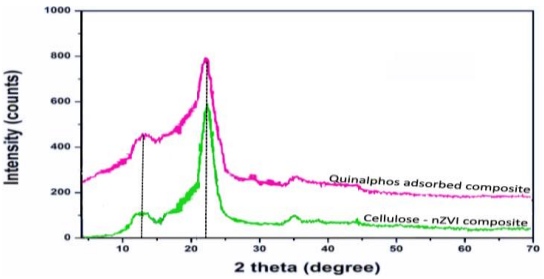


**Fig. 6: XRD pattern of the composite**

**BET surface area analysis**

The surface area of the composite was determined by nitrogen adsorption experiments (performed at 77.4 K in the Relative-pressure (P/Po) range of 0.0001–1) - (Fig. 7a). The adsorption of nitrogen elevated at higher relative pressures, testifying to the fact that the operating conditions impact the whole process of adsorption. In order to gauge the pore-size distribution of the composite, the Barrett-Joyner-Halenda (BJH) method was brought into play. The BET surface area of the composite was measured at 1.631 $m^2/g$ and its pore size at 3.634 nm. The pore-size distribution curve of the composite illustrates pore size distributions in the micropore (<2 nm) and mesopore (2–50 nm) regimes. The analysed sample showed pore-sizes in the range of 1.7 - 30 nm; hence the pores were proved to be distributed mostly in the mesoporous regime (Fig.7b).

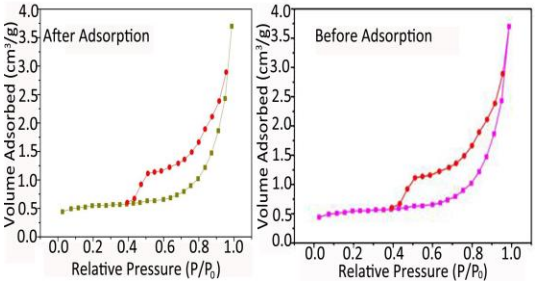


**Fig. 7a: $N_2$ adsorption- desorption isotherm for composite**

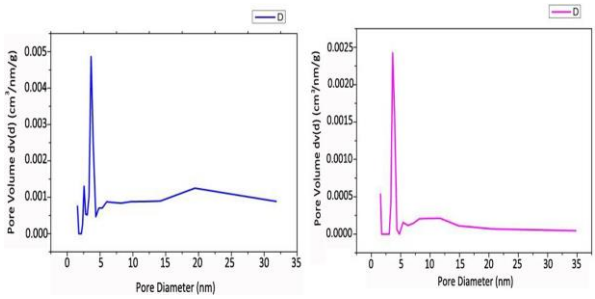


**Fig. 7b. BJH pore size distribution of the composite**

**Adsorption analysis**

**Effect of the contact time**

The capability of the nZVI/CFs composites for the elimination of quinalphos from aqueous solutions was gauged by regulating the contact time in the slot of 10–90 min range at absorbent dosage of 0.1 g in the presence of 10 mg/L content of nitrate at pH 3 and 303 K. As depicted in Fig. 8, the adsorption capacity of the nZVI/CFs composite attained the state of saturation at 60 min, and thereafter managed to remain almost unchanged. The nZVI/CFs composites turned out to be apt for adsorption of quinalphos out of a bulk solution; pesticide adsorbed onto the active-sites on the adsorbent surface and the least minimum time needed for adsorption was found to be 60 min.

**Effect of pH**

The impact of pH value on the adsorption of quinalphos onto nZVI/CFs was gauged at five different pH viz. 3, 5, 7, 9, and 11. The results shown in Fig. 8 indicate that the pH of solution has a direct influence on the adsorption of quinalphos onto nZVI/CFs, i.e. the adsorption-efficiency was higher at pH range within 0-7. The higher adsorption-capacity for low pH is predominantly owing to the strongly relevant electrostatic interaction between the positively charged sites of the adsorbent and quinalphos (Fig. 7). When the solution pH was raised, the surface became charged negatively and hence the adsorption-capacity for quinalphos dropped, as the negatively charged surface sites on the adsorbent disfavour adsorption of quinalphos owing to the electrostatic repulsion.

**Dosage of the adsorbent**

The percentage of removal for different dosages of the adsorbent viz., 0.1, 0.2, 0.3, 0.4, and 0.5 g was analyzed to determine the impact of adsorbent dosage and also to optimise the minimum dosage required for the removal of quinalphos. As depicted in Fig. 8, just as expected, the percentage of removal of quinalphos had risen significantly whenever there was a case of an increment in the adsorbent dosage, which is clearly down to the rise in the number of active sites along with the increase in the adsorbent dosage.

**Impact of the initial concentration**

The impact of the initial quinalphos concentration was investigated by adding fixed amounts of adsorbents to solutions with different quinalphos concentrations, viz., 10,20,30,30 and 50 mg $L^{-1}$. The effect of the initial concentration on the quinalphos removal-efficiency is depicted in Fig. 8, which indicates quinalphos removal-efficiency dropped with an increase in the initial concentration of quinalphos. The reason for the sharp drop with the increase in the initial concentration value of quinalphos concentration is, for a fixed adsorbent dosage, the total available adsorption sites are limited, which leads to saturation as the concentration increases.

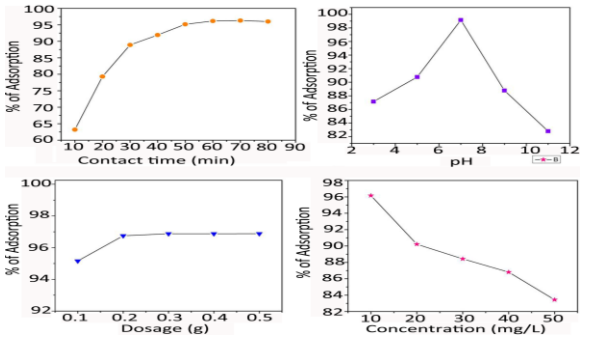


**Fig. 8: Effect of contact time, pH, dosage, and initial concentration on quinalphos**

**CONCLUSION**

The use of biosorbents based on "bio-waste" for the elimination of various pollutants from water and waste-water has numerous advantages. The adsorbents have remarkable adsorption capacity for many pollutants, and these materials are low-cost, non-toxic, and biocompatible. The present investigation was aimed at the use of a novel adsorbent, cellulose/nanoscale, zero-valent iron nanocomposite for the removal of an organothiophosphate pesticide (quinalphos) from aqueous solutions. The effects of the adsorbent dosage, solution pH, concentration, and contact time were studied. Maximum adsorption of quinalphos was achieved at 60 min. The optimum pH for maximum removal was found to be 7. The pore size distribution of the prepared composite falls in the mesoporous regime. The effective removal of quinalphos indicates the advantage of our composite over other sorbents. The prepared composites proved out to be promising materials for eliminating quinalphos from aqueous solutions. The unique properties of nanomaterials and their combination with biomaterials provide great opportunities to revolutionise water treatment.

**REFERENCES**

1. DeMarco, M.J.; Sen Gupta, A.K.; Greenleaf, J.E. Arsenic Removal Using a Polymeric/Inorganic Hybrid Sorbent. Water Res. 2003, 37(1), 164–176.
2. T.D. Lazarevi´c-Pa˘sti, A.M. Bond˘zi´c, I.A. Pa˘sti, S.V. Mentus, and V.M. Vasi´c, "Electrochemical oxidation of diazinon in aqueous solutions via electrogenerated halogens—diazinon fate and implications for its detection," *Journal of Electroanalytical Chemistry*, vol. 692, pp. 40–45, 2013.

3. S. Chiron, A.R. Fern´andez-Alba, A. Rodr´ıguez, and E. Garc´ıa- Calvo, "Pesticide chemicaloxidation: state of the art," *Water Research*, vol. 34, pp. 366–377, 2000.
4. J.G. Wu, T.G. Luan, C.Y. Lan, W.H. Lo, and G.Y.S. Chan, "Efficacy evaluation of low-concentration of ozonated water in removal of residual diazinon, parathion, methyl-parathion and cypermethrin on vegetable," *Journal of Food Engineering*, vol. 79, no. 3, pp. 803–809, 2007.
5. K. Ikehata and M.G. El-Din, "Aqueous pesticide degradation by ozonation and ozone-based advanced oxidation processes: a review (part II)," *Ozone: Science and Engineering*, vol. 27, no. 3, pp. 173–202, 2005.
6. Y. Ku, H.S. Lin, W. Wang, and C.M. Ma, "Decomposition of diazinon in aqueous solution by ozonation," *Water Research*, vol. 32, no. 6, pp. 1957–1963, 1998.
7. G. Moussavi, H. Hosseini, and A. Alahabadi, "The investigation of diazinon pesticide removal from contaminated water by adsorption onto NH4Cl-induced activated carbon," *Chemical Engineering Journal*, vol. 214, pp. 172–179, 2013.
8. V.K. Gupta, B. Gupta, A. Rastogi, S. Agarwal, and A. Nayak, "Pesticides removal from waste water by activated carbon prepared from waste rubber tire," *Water Research*, vol. 45, no. 13, pp. 4047–4055, 2011.
9. K.Y. Foo and B.H. Hameed, "Detoxification of pesticide waste via activated carbon adsorption process," *Journal of Hazardous Materials*, vol. 175, no. 1–3, pp. 1–11, 2010.
10. A. Dhaouadi, L. Monser, and N. Adhoum, "Removal of rotenone insecticide by adsorption onto chemically modified activated carbons," *Journal of Hazardous Materials*, vol. 181, no. 1–3, pp. 692–699, 2010.
11. B. Sarkar, N. Venkateswralu, R.N. Rao, C. Bhattacharjee, and V. Kale, "Treatment of pesticide contaminated surface water for production of potable water by a coagulation-adsorption nanofiltration approach," *Desalination*, vol. 212, no. 1–3,pp. 129– 140, 2007.
12. R. Boussahel, S. Bouland, K.M. Moussaoui, and A. Montiel, "Removal of pesticide residues in water using the nanofiltration process," *Desalination*, vol. 132, no. 1–3, pp. 205–209, 2000.
13. K. Koˇsuti´c, L. Furaˇc, L. Sipos, and B. Kunst, "Removal of arsenic and pesticides from drinking water by nanofiltration membranes," *Separation and Purification Technology*, vol. 42, no. 2, pp. 137–144, 2005
14. P. Trebˇse and I. Arˇcon, "Degradation of organophosphorus compounds by X-ray irradiation," *Radiation Physics and Chemistry*, vol. 67, no. 3-4, pp. 527–530, 2003.
15. Y. Gao, Y.B. Truong, P. Cacioli, P. Butler, and I.L. Kyratzis, "Bioremediation of pesticide contaminated water using an organophosphate degrading enzyme immobilized on nonwoven polyester textiles," *Enzyme and Microbial Technology*, vol. 54, no. 1, pp. 38–44, 2014.
16. R. Li, J. Zheng, R.Wang et al., "Biochemical degradation pathway of dimethoate by *Paracoccus* sp. Lgjj-3 isolated from treatment wastewater," *International Biodeterioration and Biodegradation*, vol. 64, no. 1, pp. 51–57, 2010.
17. T.A. McMurray, P.S.M. Dunlop, and J.A. Byrne, "The photocatalytic degradation of atrazine on nanoparticulate TiO2 films," *Journal of Photochemistry and Photobiology A: Chemistry*, vol. 182, no. 1, pp. 43–51, 2006.
18. Q. Wang and A.T. Lemley, "Oxidation of diazinon by anodic Fenton treatment," *Water Research*, vol. 36, no. 13, pp. 3237– 3244, 2002.
19. Y. Zhang, Y. Hou, F. Chen, Z. Xiao, J. Zhang, and X. Hu, "The degradation of chlorpyrifos and diazinon in aqueous solution by ultrasonic irradiation: effect of parameters and degradation pathway," *Chemosphere*, vol. 82, no. 8, pp. 1109–1115, 2011.
20. Y.N. Liu, D. Jin, X.P. Lu, and P.-F. Han, "Study on degradation of dimethoate solution in ultrasonic airlift loop reactor," *Ultrasonics Sonochemistry*, vol. 15, no. 5, pp. 755–760, 2008.
21. J.D. Schrammand I. Hua, "Ultrasonic irradiation of dichlorvos: decomposition mechanism," *Water Research*, vol. 35, no. 3, pp. 665–674, 2001
22. Parhi, P.K. Supported Liquid Membrane Principle and Its Practices: A Short Review. J. Chem. 2012, 2013, 11.
23. Richards, L. A.; Richards, B. S.; Schafer, A. I. Renewable Energy Powered Membrane Technology: Salt and Inorganic Contaminant Removal by Nanofiltration/Reverse Osmosis. J. Membr. Sci. 2011, 369, 188–195.
24. Kulkarni, S.J.: Advancements, research and challenges in reactive adsorption: a review. Int. J. Res. **2**(1), 477–480 (2015)
25. Siro, I.; Plackett, D. Microfibrillated cellulose and new nanocomposite materials: A review. Cellulose. 2010, 17, 459–494.
26. French, A. D., & Santiago Cintrón, M. (2013). Cellulose polymorphy, crystallite size,and the segal crystallinity index. Cellulose, 20, 583–588.
27. Driemeier, C., & Calligaris, G. A. (2011). Theoretical and experimental developmentsfor accurate determination of crystallinity of cellulose I materials. Journal ofApplied Crystallography, 44, 184–192
28. Ponnamma, D.; Sadasivuni, K. K.; Grohens, Y.; Guo, Q.; Thomas, S. Carbon Nanotube Based Elastomer Composites-An Approach Towards Multifunctional Materials. J. Mater. Chem. 2014, 2, 8446–8485
29. Lu, J.; Xu, K.; Yang, J.; Hao, Y.; Cheng, F. Nano Iron Oxide Impregnated in Chitosan Bead as a Highly Efficient Sorbent for Cr (VI) Removal from Water. Carbohydr. Polym. 2017, 173, 28–36.
30. Kolbasov, A.; Sinha-Ray, S.; Yarin, A. L.; Pourdeyhimi, B. Heavy Metal Adsorption on Solution-Blown Biopolymer Nanofiber Membranes. J. Membr. Sci. 2017, 530, 250–263.
31. Byeona, J.H.; Kim, Y.W. Continuous Gas-Phase Synthesis of Graphene Nanoflakes Hybridizes by Gold Nanocrystals for Efficient Water Purification and Gene Transfection. Chem. Eng. J. 2013, 229, 540–546.
32. Sun, X. F.; Qin, J.; Xia, P.F.; Guo, B.B.; Yang, C.M.; Song, C.; Wang, S.G. Graphene Oxide-Silver Nanoparticle Membrane for Biofoulding Control and Water Purification. Chem. Eng. J. 2015, 81, 53–59.
33. Liang, J.; Zhou, Y.; Jiang, G. H.; Wang, R. J.; Wang, X. H.; Hu, R.B.; Xi, X.G. Transformation of Hydrophilic Cotton Fabrics into Superhyd rophobic Surfaces for Oil/Water Separation. J. Text. Inst. 2013, 104, 305–311.
34. Zeng, J.W.; Wang, B.; Zhang, Y. B.; Zhu, H.; Guo, Z. G. Strong Amphiphobic Porous Films with Oily-Self Cleaning Properly beyond Nature. Chem. Lett. 2014, 43, 1566–1568. DOI: 10.1246/cl.140600.
35. Huang, J.Y.; Li, S.H.; Wang, L.N.; Xing, T.L.; Chen, G.Q.; Liu, X.F.; Al-Deyab, S.S.; Zhang, K.Q.; Chen, T.; Lai, Y.K.J. Robust Superhydrophobic TiO2 @Fabrics for UV Shielding, Self-Cleaning and Oil- Water Separation. Mater.Chem. A 2015, 3, 2825–2832.
36. Zhang, M.; Zang, D.L.; Shi, J. Y.; Gao, Z.X.; Wang, C.Y.; Li, J. Superhydrophobic Cotton Textile with Robust Composite Film and Flame Retardency. RSC Adv. 2015, 5, 67780–67786.
37. Xiong, Z.; Ma, J.; Ng, W. J.; Waite, T. D.; Zhao, X. S. Silver Modified Mesoporous TiO2 Photocatalyst for Water Purification. Water Res. 2011, 45, 2095–2103.
38. Kadam, A.A.; Lee, D.S. Glutaraldehyde Cross-Linked Magnetic Chitosan Nanocomposites: Reduction Precipitation Synthesis, Characterizations and Applications for Removal of Hazardous Textiles Dyes. J. Bioresour. Technol. 2015, 193, 563–567.
39. Li, L.; Li, Y.; Cao, L.; Yang, C. Enhanced chromium- (VI) Adsorption Using Nanosized Chitosan Fibers Tailored by Electrospinning. Carbohydr. Polym. 2015, 125, 206–213.
40. Rahmi, Lelifajri, Julinawati, Shabrina. Carbohydrate Polymers (2017).

41. Ahmed, M.E. Khalil, osama Eljammal-Journal of novel carbon resource science (2016)
42. Dufresne. A, Cavaille. J.Y, Vignon. M.R (1997). Mechanical behavior of sheets prepared from sugar beet cellulose micro fibrils. Journal of Applied Polymer Science, 64(6).1185-1194
43. Pelisari. M.F, Sobral. P.J, Menegalli. F.C (2014). Isolation and characterization on cellulose nano fibers from banana peels, Cellulose, 21(1),417
44. Sao. K, Mathew. M.D & Ray P.K (1987). Infrared spectra of alkali treated degummed Ramie. Textile Research Journal 57(7), 407-414.
45. Xu. F, Zhou, Q.A, Sun. J.X, Liu. C.F, Ren. J.L, Sun. R.C (2007). Fractionation and charecterization of chlorophyll and lignin from dejuiced Italian rye grass (Loliummultifolrum) and timothygrass (Phleumpratense). Process Biochemistry 42(5), 9.
46. Zuluaga, R, Putaux. J.L, Cruz. J, Velez. J, Mondragon. I, & Ganam. P (2009). Cellulose microfibrils from banana rachis: Effect of alkaline treatments on structural and morphological features. Carbohydratepolymer,76(1),51-59
47. Sun. J.X, Xu. F, Sun. X.F, Xiao. B & Sun. R.C (2005). Physicochemical and thermal character- risation of cellulose from barely straw. Polymer Degradation a and Stability 88(3),521-531
48. Xiao. B, Sun. X.F & Sun. R.C (2001). Chemical, structural and thermal characterization of alkali soluble ligninsand chemicellulose and cellulose from maize stems, rye straw a and rice straw. Polymer Degradation and Stability 74(2), 307-319.
49. Rajput G, Majmudar F, Patel J, Thakor R, Rajgor NB. "Stomach-Specific Mucoadhesive Microsphere as a Controlled Drug Delivery System." *Systematic Reviews in Pharmacy* 1.1 (2010), 70-78. Print. doi:10.4103/0975-8453.59515
50. Alemdar. A & Sain.M (2008b). Biocomposites from wheat straw nanofibers: Morphology, thermal and mechanical properties. Composites Science and Technology, 68(2), 557-565
51. Rosa. M.F, Medeiros, E.S. Malmonge, J.A. Gregorski, K.S. Wood, D. Fmattoso (2010). Cellulose nano whiskers from coconut huskfibers: Effect of preparation conditions on their thermal and morphological behaviour. Carbohydrate Polymer, 81 (1), 83-92.
52. Song, Z., Lehr, E., Wang, S.An alternative subcoronary implantation technique decreases the risk of complete heart block after stentless aortic valve replacement(2012) Journal of Cardiovascular Disease Research, 3 (1), pp. 46-51. DOI: 10.4103/0975-3583.91594